cluster structures occurs at $n = 6$.

The IR spectrum of the dominant R2PI transition assigned to BW_7 (Fig. 2G) further confirms this interpretation. By comparison to the BW_6 spectrum, the spectrum of BW_7 transfers additional intensity from the free O–H stretch transitions at 3713 cm^{-1} to new bands in the region from 3500 to 3600 cm^{-1} ascribable to double donor O–H stretches. Thus, already by BW_7, the majority of water molecules donate both hydrogens to hydrogen bonds.

We cannot presently distinguish which of the several low-energy noncyclic W_n structures is present in BW_6 and BW_7. In fact, the R2PI spectra of Fig. 1, E and F, show weak features that may be attributable to other structural isomers; IR spectra of these features as well as IR spectra of even larger BW_n clusters are needed. Given the large number of calculated structures with nearly the same energy [Tsai and Jordan (*17*) found 20 W_6 structures within 2 kcal/mol of the lowest energy structure], the presence of benzene may alter the energy ordering of the W_n structures. Ultimately, calculations of the IR frequencies and intensities of the BW_n clusters themselves are needed for direct comparison with experiment.

REFERENCES AND NOTES

1. G. C. Pimentel and A. L. McClellan, *The Hydrogen Bond* (Freeman, San Francisco, 1960).
2. For a recent overview of the subject, see J. C. Pore and J. Texeira, Eds., *Hydrogen-Bonded Liquids* (Kluwer, Dordrecht, Netherlands, 1991).
3. Some examples of studies of liquid water and ice: T. C. Sivakumar, S. A. Rice, M. G. Sceats, *J. Chem. Phys.* **69**, 3468 (1978); M. S. Bergren, D. Schuh, M. G. Sceats, S. A. Rice, *ibid.*, p. 3477; J. P. Devlin, in *Proton Transfer in Hydrogen-Bonded Systems*, T. Bountis, Ed. (Plenum, New York, 1992).
4. T. R. Dyke and J. S. Muenter, *J. Chem. Phys.* **60**, 2929 (1974); J. A. Odutola and T. R. Dyke, *ibid.* **72**, 5062 (1980).
5. K. L. Busarow *et al.*, *ibid.* **90**, 3937 (1989); N. Pugliano and R. J. Saykally, *ibid.* **96**, 1832 (1992).
6. N. Pugliano and R. J. Saykally, *Science* **257**, 1937 (1992).
7. E. Zwart, J. J. ter Meulen, W. L. Meerts, L. H. Coudert, *J. Mol. Spectrosc.* **147**, 27 (1991).
8. Z. S. Huang and R. E. Miller, *J. Chem. Phys.* **91**, 6613 (1989).
9. D. F. Coker *et al.*, *ibid.* **82**, 3554 (1985).
10. M. F. Vernon *et al.*, *ibid.* **77**, 47 (1982); R. H. Page, J. G. Frey *et al.*, *Chem. Phys. Lett.* **106**, 373 (1984); R. H. Page *et al.*, *ibid.* **141**, 1 (1987).
11. S. Wuelfert, D. Herren, S. Leutwyler, *J. Chem. Phys.* **86**, 3751 (1987).
12. A. Engdahl and B. Nelander, *ibid.*, p. 4831.
13. R. M. Brentwood, A. J. Barnes, W. J. Orville-Thomas, *J. Mol. Spectrosc.* **84**, 391 (1980).
14. S. S. Xantheas and T. H. Dunning Jr., *J. Chem. Phys.* **99**, 8774 (1993).
15. E. Honegger and S. Leutwyler, *ibid.* **88**, 2582 (1988).
16. R. Knochenmuss and S. Leutwyler, *ibid.* **96**, 5233 (1992).
17. C. J. Tsai and K. D. Jordan, *Chem. Phys. Lett.* **213**, 181 (1993).
18. A. Vegiri and S. C. Farantos, *J. Chem. Phys.* **98**, 4059 (1993).
19. K. S. Kim *et al.*, *Chem. Phys. Lett.* **131**, 451 (1986); B. J. Mhin *et al.*, *J. Chem. Phys.* **100**, 4484 (1994).
20. K. F. Franken, M. Jalaie, C. E. Dykstra, *Chem. Phys. Lett.* **198**, 59 (1992); C. E. Dykstra, *J. Chem. Phys.* **91**, 6472 (1989).
21. K. Laasonen, M. Parrinello, R. Car, C. Lee, D. Vanderbilt, *Chem. Phys. Lett.* **207**, 208 (1993).
22. D. Belford and E. S. Campbell, *J. Chem. Phys.* **86**, 7013 (1987).
23. J. G. C. M. van Duijneveldt–van de Rijdt and F. B. van Duijneveldt, *J. Comput. Chem.* **13**, 399 (1992).
24. K. Szalewicz, S. J. Cole, W. Kolos, R. J. Bartlett, *J. Chem. Phys.* **89**, 3662 (1988).
25. J. R. Reimers, R. O. Watts, M. L. Klein, *Chem. Phys.* **64**, 95 (1982).
26. S. Zlanina, *Z. Phys. Chem.* **171**, 131 (1991).
27. A. Engdahl and B. Nelander, *J. Phys. Chem.* **89**, 2860 (1985).
28. A. J. Gotch and T. S. Zwier, *J. Chem. Phys.* **96**, 3388 (1992); A. W. Garrett and T. S. Zwier, *ibid.*, p. 3402. See also a review chapter by A. W. Garrett and T. S. Zwier to appear in *Advances in Multiphoton Processes and Spectroscopy*, vol. 9, S. H. Lin, A. A. Villaeys, Y. Fujimara, Eds. (World Scientific, River Edge, NJ, in press).
29. S. Suzuki *et al.*, *Science* **257**, 942 (1992).
30. H. S. Gutowsky, T. Emilsson, E. Arunan, *J. Chem. Phys.* **99**, 4883 (1993).
31. J. Wanna *et al.*, *ibid.* **85**, 1795 (1986).
32. P. Linse, *J. Comput. Chem.* **9**, 505 (1988).
33. J. D. Augspurger, C. E. Dykstra, T. S. Zwier, *J. Phys. Chem.* **96**, 7257 (1992).
34. ———, *ibid.* **97**, 980 (1993).
35. R. H. Page, Y. R. Shen, Y. T. Lee, *J. Chem. Phys.* **88**, 4621 (1988).
36. BW_n clusters are formed in a pulsed supersonic expansion into which metered flows of benzene (0.1%) and water (0.2 to 0.4%) are mixed in helium at a total backing pressure of 4 bar.
37. A grating-tuned $LiNbO_3$ OPO pumped by the far-field, unseeded 1.06-μm output of a Nd:yttrium-aluminum-garnet laser (Continuum NY61-20) produces ~5 mJ per pulse over the region from 2800 to 4000 cm^{-1} of interest here. The bandwidth of the OPO is about 1 cm^{-1}.
38. R. N. Pribble and T. S. Zwier, unpublished results.
39. K. Kim and K. D. Jordan, unpublished results.

40. This work was supported by the National Science Foundation and by an equipment grant to build the OPO from Continuum, Inc. We thank K. Haber and A. Garrett for their part in the early setup of the OPO. We also thank J. Lisy for lending us a $LiNbO_3$ crystal during the early characterization of our OPO.

14 January 1994; accepted 6 April 1994

Deep Seismic Expression of an Ancient Plate Boundary in Europe

Alet Zielhuis and Guust Nolet

Seismological results on the structure of the upper mantle below Europe reveal a marked contrast in seismic properties between Precambrian and younger parts of Europe. The Precambrian craton in eastern Europe is characterized by high shear-wave velocities, which can be explained by low temperatures. The transition to low seismic velocities below Phanerozoic Europe coincides with the crustal boundary zone of the craton and exists to depths of at least 140 kilometers. Despite the long and complex tectonic history of the plate boundary zone, the transition is remarkably sharp, which rules out any significant lateral transport of asthenospheric material across the suture zone.

Western and eastern Europe have distinctly different geological histories. Precambrian eastern Europe has been stable since Late Precambrian times. In contrast, western Europe was formed during Phanerozoic accretion to the Precambrian continent. At crustal levels the boundary between the two tectonic provinces is formed by an ancient suture zone, the Tornquist-Teisseyre zone (TTZ). Stretching from south Sweden to the Black Sea, the TTZ is Europe's largest tectonic lineament. Previous seismological studies (*1*) have shown that eastern and western Europe have different upper mantle structures, but little has been known about the character, exact location, and depth of the transition between the structures. To investigate this ancient plate boundary, we discuss a detailed three-dimensional model for the shear-wave velocity in the upper mantle below Europe (*2*). This model was obtained by waveform inversion of both body and surface waves, recorded on vertical-component seismograms (*3*). Using relatively short paths and high frequencies (up to 60 MHz) we obtained a lateral resolution of about 200 km locally, which compares very favorably with the resolving power of 1000 to 2000 km in current global models of shear-wave velocity variations (*4–11*). The incorporation of higher modes of Rayleigh waves gives a depth resolution of 90 km at a depth of 80 km and 150 km at a depth of 400 km, which is superior to that of most fundamental mode studies. The three-dimensional model reveals that the TTZ is not only discernible at crustal depths but that it also forms an important boundary at upper mantle levels.

The Precambrian craton, consisting of the Baltic shield and Russian platform, is characterized by high shear-wave velocities (Fig. 1, A and B). The sharp transition to lower velocities of the Phanerozoic regions of western Europe coincides with the TTZ. Laterally, the velocity contrast

A. Zielhuis, Research School of Earth Sciences, The Australian National University, Canberra ACT 0200, Australia.
G. Nolet, Department of Geological and Geophysical Sciences, Guyot Hall, Princeton University, Princeton, NJ 08544, USA.

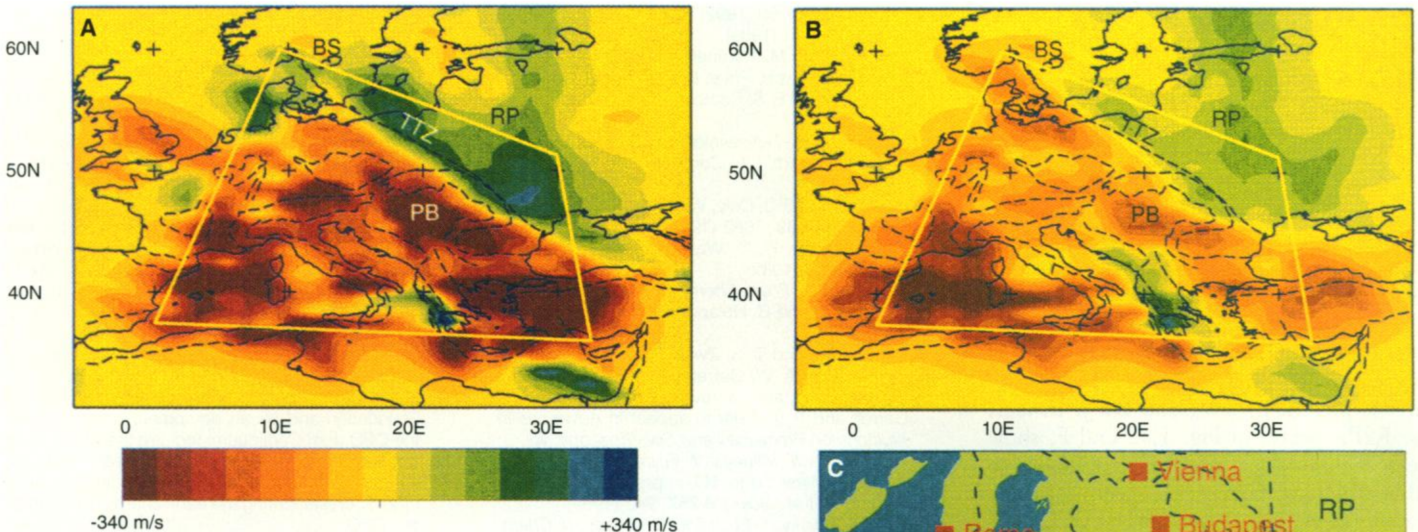

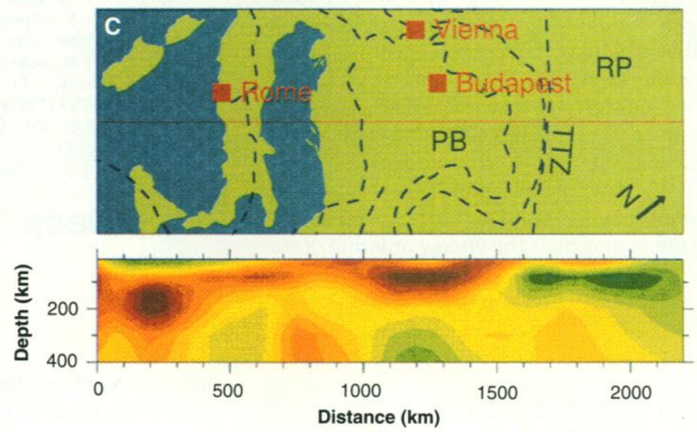

Fig. 1. (**A**) Horizontal section through the shear-wave velocity model at a depth of 80 km. The reference velocity is 4.5 km/s; velocity anomalies are contoured according to the scale bar. The Precambrian regions in eastern Europe [Russian platform (RP) and Baltic shield (BS)] are characterized by high-velocity anomalies of up to 5%. The sharp transition to the lower velocities in west and central Europe coincides with the ancient suture zone between Precambrian and Phanerozoic Europe, the TTZ. Southwest of the TTZ, velocity anomalies range from −7.5% in the Pannonian basin (PB) to about −3.5% in northern Germany and Poland. Dashed lines depict major tectonic features. The polygon bounds the region where spatial resolution is good. (**B**) Horizontal section through the velocity model at a depth of 140 km. The reference velocity is 4.5 km/s. The velocity contrast below the TTZ, the suture between Precambrian and Phanerozoic Europe, is evident at this depth. Line styles, symbols, and colors are as in (A). (**C**) (Bottom) Cross section perpendicular to the craton boundary, across the Pannonian basin and the Russian platform. Velocity anomalies with respect to a one-dimensional reference model are contoured according to the scale bar. The velocity varies over a distance of 200 km from 4.7 km/s below the Russian platform to 4.2 km/s below the Pannonian basin. (Top) Geographical map indicating the line of cross section and outlines of major tectonic elements (dashed lines).

across the suture zone varies significantly. The largest contrast (12%) is in central Europe, between the Russian platform and the Pannonian basin (Fig. 1C). The lowest contrast (5%) is in northwestern Europe, between southern Sweden and Germany (Fig. 2).

Although the ancient plate boundary zone shows no significant tectonic activity at present, our results demonstrate that it is still a prominent feature in the upper mantle. Its early history is not well understood (*12, 13*). The accretion of central and western Europe started in Late Silurian times with the collision of Avalonia (encompassing the Ardennes, England, Wales, southern Ireland, and parts of northeastern North America) and Baltica (the Baltic shield and Russian platform) after closure of the intermediate ocean, the Tornquist Sea (*14, 15*). Since then, many other micro-continents that had rifted off Gondwana collided with the southeastern boundary of Avalonia and Baltica and became part of a growing Europe. During accretion, the TTZ deformed in a stress regime that changed from strike-slip at the end of the Variscan orogeny to extension in Triassic times and transpression during the Alpine orogeny (*12, 16, 17*). Despite the strong deformation within the plate boundary zone, the Precambrian crust just east of the TTZ has remained undeformed since Early Paleozoic times (*17*). Significantly, our tomographic images reveal a relation between the size of the velocity contrast across the plate boundary zone and the time of accretion and tectonic activity west of the TTZ. In the northwest, the basement of northern Germany has been stable since the Early Paleozoic and the velocity contrast as

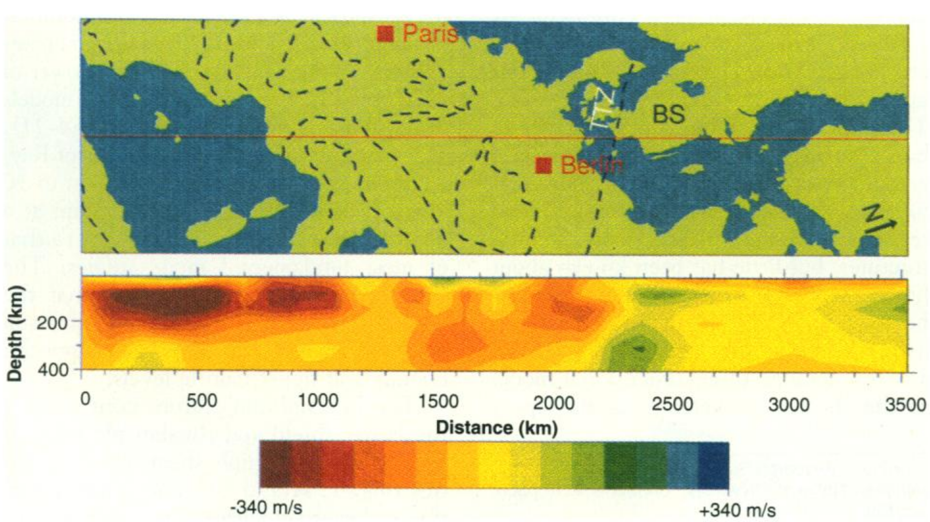

Fig. 2. Vertical section across the northwestern part of the TTZ, near south Sweden and Germany. Abbreviations are as in Fig. 1.

imaged is smaller than in central Europe, where back-arc spreading in the Pannonian basin started around the Middle Miocene during subduction along the Carpathian arc (*16, 18*).

Although a direct interpretation of the velocity contrast in terms of temperature or compositional difference is difficult (*19*), some inferences can be made by combining different sources of information. Surface heat-flow values are distinctly different on either side of the TTZ. On the Precambrian Russian platform, heat-flow values are generally less than 40 mW/m^2. In contrast, in the Phanerozoic regions heat flow is higher than 60 mW/m^2; for instance, the heat flow in the Pannonian basin exceeds 80 mW/m^2 (*20*). From heat-flow data, the temperature at a depth of 80 km below the Russian platform is estimated to be 650°C (*21*). With this temperature, the extrapolation of laboratory data (*22*) predicts a velocity of 4.72 km/s both for a pyrolite (*23*) and a piclogite (*24*) mantle composition. This value is in good agreement with the average wave speed of 4.7 km/s at a depth of 80 km below the Russian platform indicated by our tomographic model, which suggests that the high velocity below the Precambrian craton can be explained by relatively low temperatures. Because of extension and subsidence from the Neogene to the present, we cannot apply a steady-state geotherm to infer the temperature below the Pannonian basin (*25*). However, the velocity in our model is 4.2 km/s at a depth of 80 km (*26*), which is well below the velocity predicted for pyrolite and peridotite below the solidus (*22*). When the recent volcanic activity in this area is considered (*18*), the presence of partial melt is a plausible explanation for the low velocities below this region.

The increased mobility of partially molten material west of the TTZ maintains a high temperature near the craton boundary by advection. The sharpness of the velocity contrast down to at least 140 km in depth, however, rules out the lateral transport of asthenospheric material, solid or partially molten, across the TTZ. For example, in our model the distance over which the velocity changes from low to high is about 200 km (Figs. 1 and 2). This distance is at the limit of the seismic resolution and should therefore be considered as an upper value for the width of the transition zone. The characteristic distance of heat conduction is $L = \sqrt{\kappa t}$ for a thermal conductivity, κ, of $\approx 10^{-6}$ m^2/s and time t. This distance is ~100 km for a t of 400 million years (my), the time since subduction of the oceanic lithosphere of the Tornquist Sea and accretion of the first terranes to the Precambrian continent Baltica. This distance might be representative for the northwestern part of this plate boundary zone. Elsewhere, the time that passed since accretion and tectonic activity is shorter, and for a t of 100 my, L is $\approx$50 km. Both distances are compatible with the width of the boundary zone as imaged by the waveform inversion. The absence of advective heat transport across the upper plate boundary zone attests to the stability of the Precambrian craton to deep levels and forms an independent support of Jordan's hypothesis that the continental tectosphere is stabilized against destruction by convection (*27*). Below the TTZ the contrast becomes less pronounced at depths of more than about 200 km, but further to the east higher velocities extend to larger depths. This suggests a thinning of the platform edge, which is interpreted by Nolet and Zielhuis (*28*) as an effect of erosive action due to subducted volatiles.

REFERENCES AND NOTES

1. One-dimensional models for compressional velocity, shear-wave velocity, or both were derived by D. W. King and G. Calcagnile [*Geophys. J. R. Astron. Soc.* **46**, 407 (1976)]; E. Hurtig, S. Grassl, and R. P. Oesberg [*Tectonophysics* **56**, 133 (1979)]; J. W. Given and D. V. Helmberger [*J. Geophys. Res.* **85**, 7183 (1980)]; L. P. Vinnik and V. Z. Ryaboy [*Phys. Earth Planet. Inter.* **25**, 27 (1981)]; J. A. Rial, S. Grand, and D. V. Helmberger [*Geophys. J. R. Astr. Soc.* **77**, 639 (1984)]; H. Paulssen [*ibid.* **91**, 171 (1987)]; and P. Goldstein, W. R. Walter, and G. Zandt [*J. Geophys. Res.* **97**, 14097 (1992)]. The surface-wave study by R. Snieder [*ibid.* **93**, 12067 (1988)] indicated an increase in shear-wave velocities below the western boundary of the Russian platform.
2. A. Zielhuis and G. Nolet, *Geophys. J. Inter.*, in press.
3. G. Nolet, *J. Geophys. Res.* **95**, 8499 (1990).
4. G. Masters *et al.*, *Eos* **73**, 201 (1992).
5. B. Romanowicz, G. Roult, T. Kohl, *Geophys. Res. Lett.* **14**, 1219 (1987).
6. W. J. Su *et al.*, *Eos* **73**, 201 (1992).
7. J. H. Woodhouse and A. M. Dziewonski, *J. Geophys. Res.* **89**, 5953 (1984).
8. J.-P. Montagner, *Ann. Geophys. B* **4**, 283 (1986).
9. ______ and T. Tanimoto, *J. Geophys. Res.* **96**, 20337 (1991).
10. Y. Zhang and T. Tanimoto, *Nature* **355**, 45 (1992).
11. ______, *J. Geophys. Res.* **98**, 9793 (1993).
12. BABEL Working Group, *Geophys. Res. Lett.* **18**, 1091 (1991).
13. EUGENO-S Working Group, *Tectonophysics* **150**, 253 (1988).
14. C. R. Scotese and W. S. McKerrow, in *Palaeozoic and Palaeogeography and Biogeography*, W. S. McKerrow and C. S. Scotese, Eds. (Geological Society, London, 1990), pp. 1–21.
15. T. H. Torsvik, O. Olesen, P. D. Ryan, A. Trench, *Geophys. J. Inter.* **103**, 261 (1990).
16. A. Ziegler, *Geological Atlas of western and central Europe* (Shell Internationale Petroleum Maatschappij B. V., The Hague, Netherlands, 1982).
17. R. M. Pegrum, in *Petroleum Geology of the North European Margin*, A. M. Spencer *et al.*, Eds. (Graham and Trotham, London, 1984), pp. 359–369.
18. J. Dercourt *et al.*, *Tectonophysics* **123**, 241 (1986); C. Szabo *et al.*, *ibid.* **208**, 243 (1992); L. Csontos *et al.*, *ibid.*, p. 221.
19. There is a shortage of laboratory measurements of seismic velocities and their temperature and pressure derivatives in rock-forming minerals (*22*). Moreover, there could be a fundamental ambiguity because the derivatives published are usually determined at ultrasonic frequencies and may not be correct at the lower seismic frequencies. For instance, anelastic relaxation at high subsolidus temperatures may result in enhanced temperature sensitivity of the elastic wave speeds [C. Goetze, in *High Pressure Research*, M. H. Manghnani and S. Akimoto, Eds. (Academic Press, New York, 1977), pp. 3–23; I. Jackson, M. S. Paterson, J. D. Fitz Gerald, *Geophys. J. Inter.* **108**, 517 (1992); S. Karato, *Geophys. Res. Lett.* **20**, 1623 (1993); I. Jackson, personal communication, 1993]. In addition, there is uncertainty in the amplitude of the variations in shear-wave speed determined in our study because of damping and smoothing applied in the inversion.
20. V. Cermak and E. Hurtig, enclosure in *Terrestrial Heat Flow in Europe*, V. Cermak and L. Rybach, Eds. (Springer-Verlag, Berlin, 1979).
21. H. N. Pollack and D. S. Chapman, *Tectonophysics* **38**, 279 (1977).
22. T. S. Duffy and D. L. Anderson, *J. Geophys. Res.* **94**, 1895 (1989).
23. A. E. Ringwood, *Composition and Petrology of the Earth's Mantle* (McGraw-Hill, New York, 1975).
24. D. L. Anderson, *Theory of the Earth* (Blackwell, Boston, 1989), pp. 45–62.
25. P. Morgan and W. D. Gosnold [*Geol. Soc. Am. Mem.* *172* (1989), pp. 493–522] give an overview of the difficulties in relating geotherms to heat-flow data for tectonically active regions of the western United States. Because deformation of the lithosphere occurs at a rate faster than heat can be transferred by conduction, vertical movement of the lithosphere results in thermal convection of heat. For instance, the effect of Neogene uplift and lithospheric thinning of the Colorado plateau is not yet noticeable in the surface heat flow [P. Morgan and C. A. Swanberg, *J. Geodyn.* **3**, 65 (1985)]. One can envisage similar effects for the Pannonian basin (PB), with Miocene extension and current subsidence rates at 160 mm/year [F. Horvath and H. Berckhemer, in *Alpine-Mediterranean Geodynamics*, H. Berckhemer and K. Hsu, Eds., Vol. 7 of *Geodynamics* series (American Geophysical Union, Washington, DC, 1982), pp. 141–173]. Effects of extension have been taken into account for models of the geotherm below the Basin and Range province (BR) [A. H. Lachenbruch and J. H. Sass, *Geol. Soc. Am. Mem.* *152* (1978), pp. 209–250], which resembles the PB qua heat flow (85 mW/m^2) and crustal thickness (both 30 km). These intersect the dry-basalt solidus between 45 and 50 km in depth. This geotherm is, however, not applicable to the PB because (i) the amount of extension is different (10 to 35% in PB) [F. Horvath and H. Berckhemer, in *Alpine-Mediterranean Geodynamics* (above), pp. 141–173] against 100% (locally 200%) in BR [R. E. Anderson, *Geol. Soc. Am. Mem.* *172* (1989), pp. 163–176] and (ii) the extension history is different: In PB, extension started around the Middle Miocene (*18*), whereas BR had main extension 40 to 50 my ago (R. E. Anderson, *ibid.*, pp. 163–176).
26. R. Snieder [in (*1*)] reported the same value. Also, low compressional wave velocities are found beneath depths of about 60 km [V. B. Sollogub *et al.*, *Tectonophysics* **20**, 1 (1973); W. Spakman, S. Van der Lee, R. D. Van der Hilst, *Phys. Earth Planet. Inter.* **79**, 3 (1993)].
27. T. H. Jordan, *Nature* **274**, 544 (1978).
28. G. Nolet and A. Zielhuis, *J. Geophys. Res.*, in press.

29. The shear-wave velocity model was produced during the PhD research of A.Z. at the University of Utrecht in the Netherlands, which was funded by the Dutch organization for the Advancement of Pure Research (NWO). A significant part of the data was obtained through the Observations and Research Facilities for European Seismology (ORFEUS) and Incorporated Research Institutions for Seismology (IRIS) data centers. We thank I. Jackson for discussions about the temperature derivatives of shear wave velocity and R. Van der Hilst for discussions and for critically reading the manuscript.

27 December 1993; accepted 11 April 1994